ABSTRACT

MORCKEL, ALLISON REBECCA. Light Activated Modulation of Protein Activity in Living Embryos. (Under the direction of Dr. Nanette Nascone-Yoder).

Small molecule inhibitors are valuable tools for elucidating protein function during embryonic development and organogenesis. For example small molecule inhibitors of Rho kinase perturb digestive tract elongation in embryos of the frog *Xenopus laevis,* implicating Rho GTPase signaling in the morphogenesis of the primitive gut tube. Although such chemical tools are effective for controlling target protein activity over time, achieving spatial control over such compounds would be of even greater utility and would facilitate finer resolution of the role of target proteins in specific tissues. In this thesis, a methodology for achieving light-controlled inhibition of Rho kinase activity was developed. A novel photoactivatable derivative of the small molecule Rho kinase inhibitor "Rockout,"was found to disrupt signaling in a defined region of living *Xenopus* embryos in response to exposure to ultraviolet light (UV). By varying the concentration of the caged compound to which the embryos are exposed prior to UV exposure, the length of time the embryos are equilibrated in the compound, or the length of time the region of interest is exposed to UV light, localized rho kinase-dependent defects can be elicited in specific regions of the developing digestive tract with minimal non-specific side effects to neighboring tissues. Photoactivatable small molecules are therefore convenient tools for light activated modulation of protein activity in specific tissues and organs in living embryos.

Light Activated Modulation of Protein Activity in Living Embryos

by
Allison Rebecca Morckel

A thesis submitted to the Graduate Faculty of
North Carolina State University
in partial fulfillment of the
requirements for the degree of
Master of Science

Comparative Biomedical Sciences

Raleigh, North Carolina

2011

APPROVED BY:

Dr. Nanette Nascone-Yoder Co-chair of Advisory Committee	Dr. Jeff Yoder Co-chair of Advisory Committee
Dr. Mac Law	Dr. Alex Deiters

DEDICATION

I dedicate this thesis to my family, friends, and amazing dog Mr.P (Parker), all of whom have supported me throughout this process.

BIOGRAPHY

I was born and raised in Winston-Salem, North Carolina where I graduated from Parkland High School in 2003. After beginning my undergraduate career at Pepperdine University I transferred to North Carolina State University in Raleigh where I received my B.S. in Biological Sciences and minor in Genetics in 2007.

ACKNOWLEDGMENTS

I would like to thank my advisor Dr. Nanette Nascone-Yoder for all that she has taught me. Her guidance has helped me through many challenges I faced in graduate school. I would also like to thank my committee members, Dr. Jeff Yoder, Dr. Mac Law, and Dr. Alex Deiters for all of their input. In addition there are several undergraduate and graduate lab members in Dr. Nascone-Yoder's lab who provided valuable insight that I would like to thank. Lastly, I would like to thank my family and friends for all of their support and encouraging words. I would not be this woman without them.

TABLE OF CONTENTS

LIST OF FIGURES

Introduction

Chemical Genetics

Chemical genetics, the use of small molecules (carbon-containing compounds of low molecular weight, i.e., <500) to examine biological processes, has become a vital tool in research. In a standard genetic screen, the phenotypes caused by random mutation of an organism identifies individuals with defects in a developmental process and subsequently can be used to identify which gene was disrupted to cause the mutant phenotype (Stockwell, 2000; Kawasumi & Nghiem, 2007). In contrast, in chemical genetic screens exogenous small molecules are screened for having a desirable biological activity in biochemical assays, or eliciting abnormalities resembling mutant phenotypes in whole organisms, and then the cellular protein targets of the small molecule can be identified (Stockwell, 2000; Yeh & Crews, 2003; Kawasumi & Nghiem, 2007).

Small molecules have provided valuable insight into the mechanisms, targets, and pathways of endogenous molecules in many organisms. For example, a high-throughput kinase assay identified the organic compound PD 184352 as an inhibitor of MEK1 kinase activity (Sebolt-Leopold et al., 1999). The compound was specific for MEK1 in that it did not affect the activity of any other kinases tested. Researchers then examined the function of MEK1 in the behaviors of colon tumor cells. It was determined that MEK1 plays a role in cell cycle progression as well as cell morphology. Moving into the context of a whole organism, PD 184352 shrunk the size of colon tumors in mice (Sebolt-Leopold et al., 1999). [When researchers attempted to create Mek-1 deficient mice, embryos died early in

embryogenesis thus precluding the use of Mek-1 deficient adult mice for studying the role of MEK1 *in vivo* (Giroux et al., 1999)]. In this study, a novel small molecule inhibitor of MEK1 was invaluable for examining the function of MEK1 in tumor formation *in vivo*.

Thus, where classical genetic loss-of-function techniques lack conditionality, cell permeable small molecules can be used to study the role of their target proteins with precise temporal control in both tissue culture and whole organisms (Stockwell, 2000; Yeh and Crews., 2003; Kawasumi et al., 2007; Ouyang et al., 2010); however, even with the increased temporal control afforded by small molecules, methods for controlling their spatial activity are still limited. Spatial control would allow precise perturbation of protein activity in a specific organ or site of the embryo instead of the global perturbation that occurs with conventional genetic techniques.

Light Control of Biologically Active Molecules

Light control over biologically active molecules is an excellent way to interrogate intracellular mechanisms with both temporal and spatial precision (Mayer and Heckel, 2006; Goeldner and Givens, 2005; Goard et al., 2005). Photocaging is one strategy for making molecules light-responsive in which a “caging” group is attached to the molecule of interest at a site that renders that molecule temporarily inactive. Upon UV irradiation, the caging group is relinquished, thus irreversibly returning the molecule of interest to its normal biological activity (Young and Deiters, 2007; Goard et al., 2005). A general decaging/photoactivation scheme is shown in Figure 1 below:

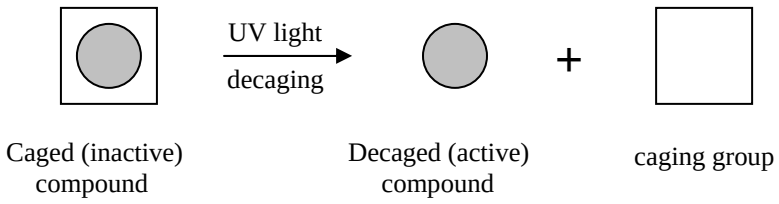

Figure 1. Decaging Scheme. In a general decaging/photoactivation scheme, the "caging group" is irreversibly relinquished upon UV irradiation thus rendering the active compound.

Another approach for making light-responsive molecules is the use of photoswitches in which the biologically active molecule is switched, reversibly, between active and inactive states (Mayer and Heckel, 2006). Upon UV irradiation the molecule is opened to its active form, but then returns to its inactive form in the dark or in response to visible light irradiation (Givens et al., 1998; Mayer and Heckel, 2006).

Many types of molecules have been photocaged, or made "light-responsive", for biological applications including small molecules, proteins, and nucleic acids. One of the most frequently caged small molecules used to date is ATP (adenosine triphosphate), a carrier of chemical energy in living organisms which is involved in many dynamic processes such as active transport, muscle contraction, and exocytosis (Goeldner and Givens, 2005; Marriott, 1998; Kaplan et al., 1978). Neurotransmitters, such as glutamate and serotonin, have been caged as well and used to analyze receptor kinetics and other highly spatially and temporally regulated processes (Mayer et al., 2006; Maier et al., 2005; Takaoka et al., 2004; Takaoka et al., 2003; Callaway et al., 2002; Pelliccioli et al., 2002; Dorman et al., 2000). Lee et al. developed a caged dopamine and used it to investigate the autoinhibitory effect of

dopamine concentration on endogenous dopamine synthesis (2002). The Koh lab was one of the first groups to use a "caged" small molecule, estradiol, in an inducible gene control system (Link et al., 2005; Lin et al., 2002; Cruz et al., 2000). Dore's lab created a caged variant of anisomycin to inhibit protein expression in cell culture (Goard et al., 2005). Neveu and colleagues (2008) have also successfully used a caged retinoic acid in the zebrafish embryo. These studies illustrate that it is possible to incorporate photochemical control in cell culture studies and complex organisms to investigate biological processes.

Various caging groups have been developed to facilitate photochemical control. One commonly used caging group, *ortho*-nitrobenzyl and derivatives (Young and Deiters, 2007; Bochet, 2002), is effective but has the disadvantage of forming a harmful byproduct, nitrosoaldehyde, upon photoactivation (Mayer et al., 2006; Pelliccioli et al., 2002; Corrie et al., 2003). An alternative group, NPP, renders a less harmful nitrostyryl species upon photolysis (Mayer et al., 2006; Walbert et al., 2001). Other caging compounds, like DMACM, which releases its active compound within nanoseconds of activation (Hagen et al., 2003), and pHP (ketoprofen derived caging group) (Conrad II et al., 2000; Zhang et al., 1999; Park et al., 1997), are based on the coumarin system (Mayer et al., 2006; Takaoka et al., 2004; Suzuki et al., 2003; Takaoka et al., 2003; Pelliccioli et al., 2002; Furuta et al., 1999; Furuta et al., 1998; Adams and Tsien, 1993). Although there are an increasing number of effective caging groups, many have not been tested *in vivo*.

The photoprotecting group, 6-nitropiperonyloxymethyl (NPOM), is also a novel caging group (Lusic et al., 2006; Lusic et al., 2007). This NPOM compound is useful for

caging nitrogen heterocycles, and does not use the carbamate linkage that is typically used in other photolabile groups (Berry et al, 2008; Lusic et al, 2007; Lusic et al., 2006). The bulky NPOM group is released quickly upon irradiation of ~365nm, a wavelength that has been shown to be non-damaging to tissue of developing zebrafish embryos for minimal lengths of time (<12 minutes; Dong et al., 2007) and allows for precise control of activation in which natural lighting will not prematurely activate the compound.

Rho Signaling

Rho GTPases are important GTP-binding proteins, belonging to the Ras superfamily, that play key roles in various mechanisms and cellular processes involved in organ morphogenesis and embryonic development (Fritz, 2006; Etienne-Manneville et al., 2002; Settleman, 2001). They are commonly referred to as molecular switches because Rho GTPases cycle between a GDP-bound inactive state and a GTP-bound active state (Symons et al., 2000). Some of the cell behaviors regulated by Rho GTPases include cell proliferation, apoptosis, and motility (Schlessinger et al., 2009; Raftopoulou et al., 2004; Riento et al., 2003). In addition, Rho GTPases are known to regulate the actin cytoskeleton and microtubule networks in motile responses such as phagocytosis and neurite extension (Raftopoulou et al., 2004; Riento et al., 2003; Etienne-Manneville et al., 2002; Symons et al., 2000).

In the Rho signaling cascade shown below, Rho (in its active GTP bound form) binds to the Rho binding domain on Rho Kinase (ROCK). This opens the kinase's conformation, allowing ROCK to use its catalytic activity to phosphorylate downstream effectors (Amano

et al., 2000). This leads to myosin light chain (MLC) activation, causing cellular shape changes, contractility, and movement. ROCKs are protein serine/threonine kinases that play numerous roles in development, from cell migration and wound healing to heart disease and cancer (Riento et al., 2003; Redowicz, 1999).

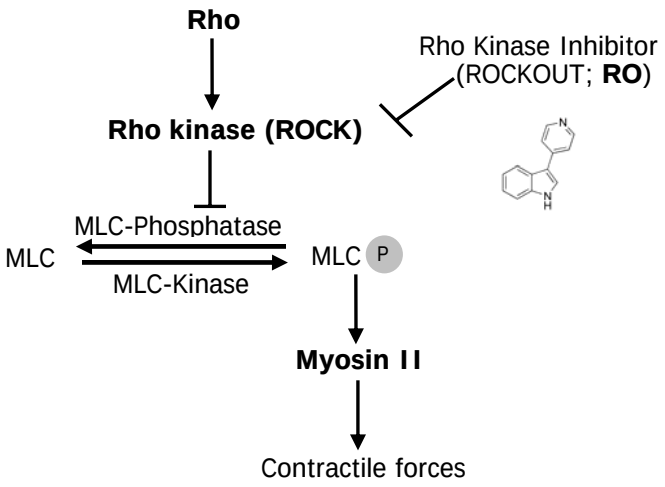

Figure 2. Rho Signalling Cascade. Rho (in its active GTP bound form) binds to the Rho binding domain on Rho Kinase (ROCK). This opens the kinase's conformation, allowing ROCK to use its catalytic activity to phosphorylate downstream effectors (Amano et al., 2000). This leads to myosin light chain (MLC) activation, causing cellular shape changes, contractility, and movement.

Since ROCKs are involved in the regulation of vital components of development and cellular motility, these proteins and inhibitors have become potential targets for novel anticancer drugs (Fritz, 2006; Riento et al., 2003). Several small molecule ROCK inhibitors with high specificity have been synthesized and used in multiple cells and organisms to elucidate the key roles of Rho GTPase signaling in development and physiological events. These inhibitors include Y-27632, H89, fasudil hydrochloride (HA1077), and 3-(4-pyridyl)indole (Rockout; **RO**). Yarrow and colleagues (2005) discovered **RO** (structure

shown above) during a phenotypic screening for cell migration inhibitors (Soderholm et al., 2005). With the known roles of Rho GTPase signaling in cell movement and contractility, Rho kinase inhibitors like **RO** can be pivotal for investigating developmental events in a wide range of organisms.

Gut Morphogenesis

Various Rho-mediated cellular and molecular mechanisms that direct cell shape, polarity, and movement are responsible for the development of the gut. The primitive gut begins as a straight tube then morphs into an elongated and rotated form. Rho GTPase signaling appears to play an important role in gut morphogenesis. For example, mutant mice lacking components upstream of Rho signaling showed defects in midgut elongation (Cervantes et al., 2009). In another study, ROCK mutant mice exhibited a defect known as omphalocele in which fusion of the body wall fails because the midgut does not return to the abdomen after elongation, however; difficulties in studying the role of ROCK in gut morphogenesis in these mice arise because the mothers inadvertently eat the protruding guts of the afflicted young with the placenta at birth (Shimizu et al., 2005; Thumkeo et al., 2005).

Rho/ROCK signaling is also involved in gut morphogenesis in other vertebrates. It has been shown that *Xenopus laevis* embryos treated globally with **RO** lack appropriate endoderm cell rearrangements and the gut fails to elongate, suggesting that Rho activity is required for the cell rearrangements that drive gut morphogenesis (Reed et al., 2009). While genetic mutants and small molecule inhibition have provided valuable insight into the mechanisms and signals controlling gut development, localized control over a small molecule

inhibitor like **RO** would help with resolving finer details of cell behaviors during gut morphogenesis. The potential roles of Rho signaling in precise positions along the entire length of the gut, such as in the formation of concavities versus convexities, or on the left versus right sides of the asymmetric coils of the gut tube, are unclear.

I hypothesize that a photoactivatable (NPOM-caged) small molecule Rho Kinase Inhibitor (**cMRO**) can be applied to *Xenopus laevis* embryos to achieve spatial control over ROCK activity during gut morphogenesis.

Experimental Methods

Embryo Culture

Xenopus laevis embryos were obtained using *in vitro* fertilization (IVF) procedures. Adult female *Xenopus laevis* were injected to target the dorsal lymph sacs with 500-800 units of Human Chorionic Gonadotropin (Sigma-Aldrich; 10,000 I.U. per vial reconstituted in 10cc's sterile water). Full ovulation is induced and females are massaged along the sides to extract eggs. The eggs are then fertilized with a small piece of a testis (previously removed from a *Xenopus* male and stored in 1X MMR) that is macerated then spread along the surface of the eggs. The eggs are covered with 0.1X MMR (Modified Marc's Ringers; Sive et al., 1998) media solution and incubated at 16-23ºC until the first cell division. Upon cleavage, embryos were carefully de-jellied of their protective jelly coat using 2% (w/v) L-cysteine pH 7.8-8.0. Embryos were staged according to Nieuwkoop and Faber developmental stages (1994).

Microinjection

A plasmid encoding EosFP (gift from F. Oswald, Wacker et al.,2007), was linearized with Not1 and used to generate synthetic capped EosFP transcripts by *in vitro* transcription (mMESSAGE mMACHINE SP6 kit; Ambion). A fluorescent dextran (dextran, cascade blue; Invitrogen, D1976; 10, 000 MW; 25 mg/mL in DEPC water) was mixed with EosFP to facilitate visualization of the injection solution during microinjections. The RNA was mixed with dextran at a ratio of 1:0.3. To target the gastrointestinal tract tissue, ~0.4ng of EosFP mRNA were injected in both the left and right sides of a 2- to 4-cell stage embryo using a pressure microinjector (WPI). Embryos with a normal phenotype (~st.37) that expressed green fluorescence over the entire gut were chosen for chemical treatment.

Photoactivation Experiments

Rockout (**RO**), **MRO**, **cMRO**, and the NPOM-caging group were generous gifts of the Deiters lab, NCSU Chemistry (see Results for synthesis scheme). Stocks of compounds were prepared in DMSO at 20mM and diluted at a range of concentrations from 1μM to 40μM for a range of equilibration times (see Results). Additionally, in order to obtain maximum solubility of **cMRO**, N-N-dimethylformamide (DMF) was combined with the compound prior to dispensing in the treatment dishes. All experiments were performed in the dark, to prevent premature photoactivation of the reagents. The general photoactivation experiment involved equilibrating *Xenopus* embryos at a stage before overt gut morphogenesis (st.37-39; Nieuwkoop and Faber, 1994) in 0.1X MMR media containing compound (**cMRO** or control) at 18.5-23ºC. The embryos were then transferred to 0.1X MMR media containing anesthetic

(5% Tricaine methanesulfonate; MS-222; Sigma) for UV irradiation (~365nm) using a Zeiss Lumar Microscope with a 1.2X lens, before being placed in fresh media to develop at 16-23ºC until scoring at the end stages of gut development (~st.43-45; See Results for more details).

Immunohistochemistry

When control embryos reached stage 42, embryos were scored, photographed, and some were processed for Immunohistochemistry (IHC) using a slightly altered staining protocol of Fagotto and Gumbiner (1998) as previously described (Reed et al., 2009). Embryos were fixed by taking the samples through five four-minute incubations in Dent's fixative (80% methanol, 20% DMSO). The embryos were then subjected to 3 washes of 1X PBS, transferred to 15% sucrose/15% gelatin, incubated at room temperature overnight, and then transferred to 15% sucrose/7.5% gelatin for another overnight incubation at room temperature. Embryos were then transferred to embedding medium, O.C.T. (Optimal Cutting Temperature) compound, frozen over dry ice and then stored at -80ºC until performance of frozen tissue sectioning on a cryostat. Primary antibodies used were anti-β-catenin (Sigma, C2206; 1:2,000), and anti-Smooth Muscle Actin (Sigma, A5228; 1:1,000). The Alexa-conjugated secondary antibodies used were Alexa488 (Invitrogen, A11029; 1:2,000) and Alexa555 (Invitrogen, A21429; 1:2,000).

Kinase Assay

Levels of Rho Kinase activity were measured with a Rho Kinase Assay Kit (Cat# CY-1160) from Cyclex with purified human Rho Kinase II (Cyclex Cat# CY-E1160-1). The detailed

protocol accompanying the kit was followed using **cMRO** and **RO** compounds at 40μM (plus and minus UV irradiation), and the purified Rho Kinase II diluted 1:20. Each sample was assayed in triplicate and the average of each group as well as standard deviation within the group was calculated in Microsoft Excel.

Liquid Chromatography-Mass Spectometry (LC/MS)

Following photoactivation experiments, gastrointestinal tracts were dissected out of embryos at the end stage of gut development (~stage 45-46). Excess liquid was removed before adding acetonitrile solvent and crushing up the gut tissue with immediate placement onto dry ice. After three cycles of freeze/thaw plus vortex agitation the samples were spun in a centrifuge at 14,000 rpm at 4ºC for 10-15 minutes. The clear supernatant (in between the froth and pellet) was collected and stored at -80ºC. Samples were processed at the Genomic Sciences Lab (GSL) facility at NCSU (by Dr. Norm Glassbrook), to determine the quantities of **RO**, **MRO**, and **cMRO** present by LC-MS analysis.

Results

Recently, Deiters et al. (2010) showed that phototactivation of NPOM-caged reagents is effective in *Xenopus* embryos. Therefore, an NPOM-caged version of the commercially available Rho Kinase Inhibitor III "Rockout" (**RO**; Calbiochem, Cat#555553), hereafter referred to as "**cMRO**", was synthesized (by the laboratory of Alex Deiters, NCSU Chemistry).

Synthesis of MRO

The synthesis of 3-(pyridin-4-yl)-1H-indole (Rockout; **RO**; Figure 3 B) was accomplished according to the method by Deubel and coworkers (1971). Benzoyl chloride was added to pyridine at –20 °C, to form an electrophilic intermediate with pyridine. Subsequent addition of indole resulted in a nucleophilic attack by the indole 2-carbon on the pyridine ring. The reaction afforded Rockout (**RO**; Figure 3 B) in 46% yield. **RO** was then transformed into [3-(pyridin-4-yl)-1H-indol-1-yl] methanol (hereafter referred to as "**MRO**"; Figure 3 C) (76% yield) by reacting it with formalin in alkaline ethanolic solution (Fraenkelconrat et al., 1947).

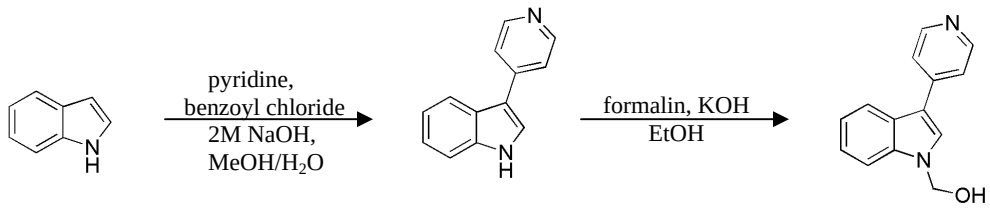

Figure 3. MRO Synthesis Scheme. The Deiters lab synythesized MRO by first adding Benzoyl chloride to pyridine at –20 °C, in order to form an electrophilic intermediate with pyridine. Subsequent addition of indole resulted in a nucleophilic attack by the indole 2-carbon on the pyridine ring. **RO** was then transformed into [3-(pyridin-4-yl)-1H-indol-1-yl] methanol (hereafter referred to as "**MRO**"; C) by reacting it with formalin in alkaline ethanolic solution

Synthesis and Decaging of cMRO

The caged ROCK inhibitor (**cMRO**; Figure 4 C) was synthesized by deprotonating with NaH in THF at –78 °C, followed by the addition of the caging group 5-[1-(chloromethoxy)ethyl]-6-nitrobenzo[d][1,3]dioxole (NPOM-Cl; Figure 4 A) . The NPOM-

caging group (blue structure; see Scheme 3) was installed on the heterocyclic nitrogen previously determined to be important for **RO** activity (Yarrow et al., 2005). The **cMRO** (Figure 4 C) was obtained in 47% yield. The low yield in formation of **cMRO** (Figure 4 C**)** matched previous observations in Deiter's lab during the course of their work with caged heterocycles (unpublished data). Deiter's and colleagues attributed these low yields to side-reactions occuring at the carbons of the indole ring system (Joule and Mills, 2000; Sundberg, 1970). However, optimization of reaction conditions for caging of indole derivatives, has not yet been undertaken. It is possible that the overall reaction yield could be improved by screening different reaction conditions (base, solvent, and temperature).

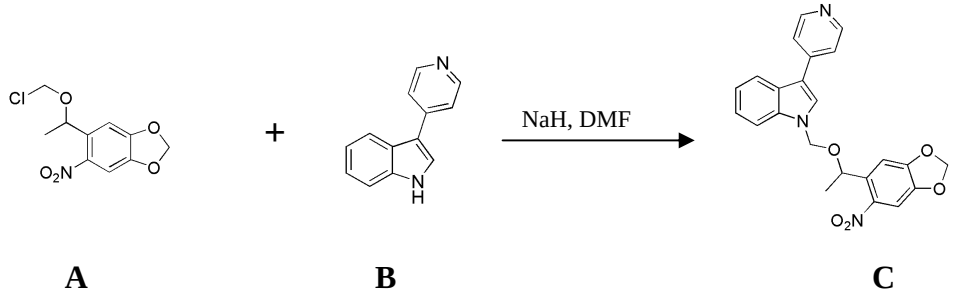

A **B** **C**

Figure 4. cMRO Synthesis Scheme. The Deiters lab synthesized cMRO by deprotonating **(**RO; B) with NaH in THF at −78 °C, followed by the addition of the caging group 5-[1-(chloromethoxy)ethyl]-6-nitrobenzo[d][1,3]dioxole (NPOM-Cl; A) .

The **cMRO** was tested for decaging at 365 nm UV irradiation. A solution of 0.1 mM caged 1-{[1-(6-nitrobenzo[d][1,3]dioxol-5-yl)ethoxy]methyl}-3-(pyridin-4-yl)-1H-indole **(cMRO;** Figure 5) was irradiated for 15 min using a hand-held UV-lamp (23 W; Spectroline). Decaging of **cMRO** (Figure 5) was monitored by HPLC/MS. Although shorter irradiation times might be sufficient, complete decaging was observed for the caged

compound after 15 min of UV irradiation. The **cMRO** decaged to **MRO** (Figure 5). Additionaly, **cMRO** also proved stable to hydrolysis at pH 7.4.

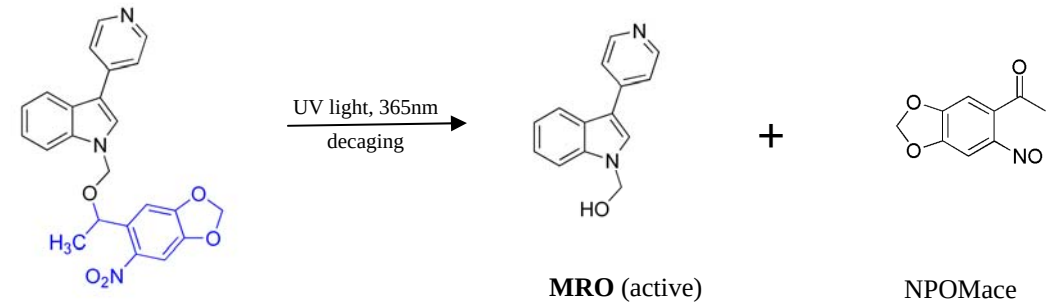

cMRO (inactive)

MRO (active)

NPOMace
Caging group

Figure 5. cMRO Decaging Scheme. Upon 365 nm UV light irradiation ,the caging group (shown in blue) of cMRO (inactive) is replaced by a proton yielding MRO (active).

Activity of Caged ROCK Inhibitor is UV-Dependent

To confirm that **cMRO** effectively blocks ROCK activity in a light-dependent manner, the ability of these compounds to inhibit ROCK activity was tested in an *in vitro* assay with purified human ROCK (Figure 6). As expected, upon treatment with **RO**, ROCK activity was reduced by ~62% in this assay. In the absence of UV irradiation, **cMRO** did not affect ROCK activity; however, two minutes UV exposure of the **cMRO** compound severely diminished ROCK activity (decreased by 90%) in this assay. These results confirm that inhibition of ROCK activity can be controlled in a photoactivatable manner by NPOM caging.

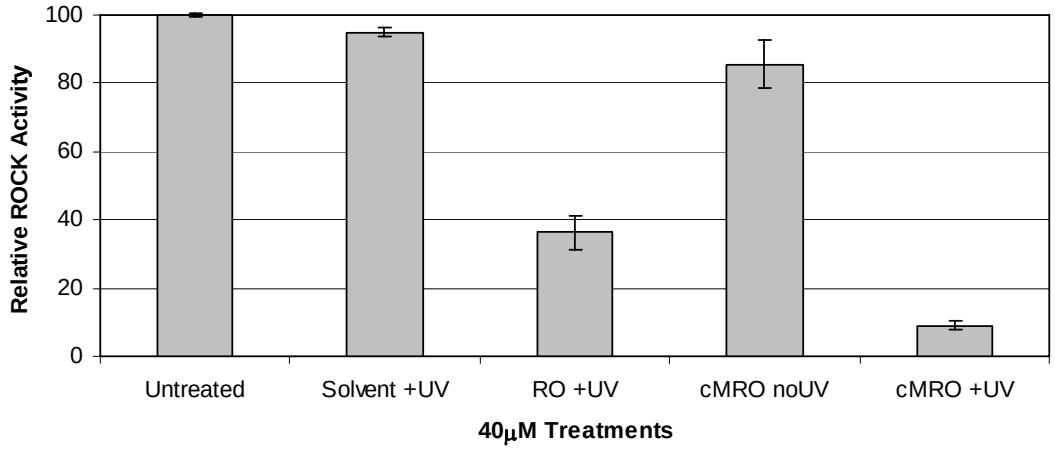

Figure 6. ROCK activity is modulated by photoactivation of cMRO. Solvent, **RO**, and **cMRO** were UV irradiated (+UV) or mock irradiated (noUV) then added to purified human ROCK at a final concentration of 40μM (or equivalent) and ROCK activity was measured (by ELISA) using an *in vitro* Rho-Kinase Assay Kit. Absorbance was measured at 450nm for each sample. Each sample was assayed in triplicate then averaged, thus error bars are representative of standard deviation.

To test whether ROCK inhibition can be photoactivated *in vivo*, embryos were equilibrated in the compounds before being exposed to UV light (Figure 7; see also Methods, "photoactivation experiments"). For long term exposures (~3days), embryos were continuously incubated in the compounds in complete darkness from a stage prior to development of the gut (st.37-39) to scoring stage (st. 43-45). For short term exposures, embryos were exposed to the compounds in the dark for a set equilibration time (0.5-4 hours), then transferred into 0.1X MMR plus anesthetic and individually irradiated or mock irradiated (no UV; kept in dark) with UV light on either the left or right side of the prospective gut, then rinsed in 0.1XMMR and cultured at 16-23ºC in the dark until scoring stage (st.43-45). The negative control groups used were 0.1XMMR and solvent whereas

positive control groups used were **RO** and **MRO**. Appropriate solvent controls were used in all experiments.

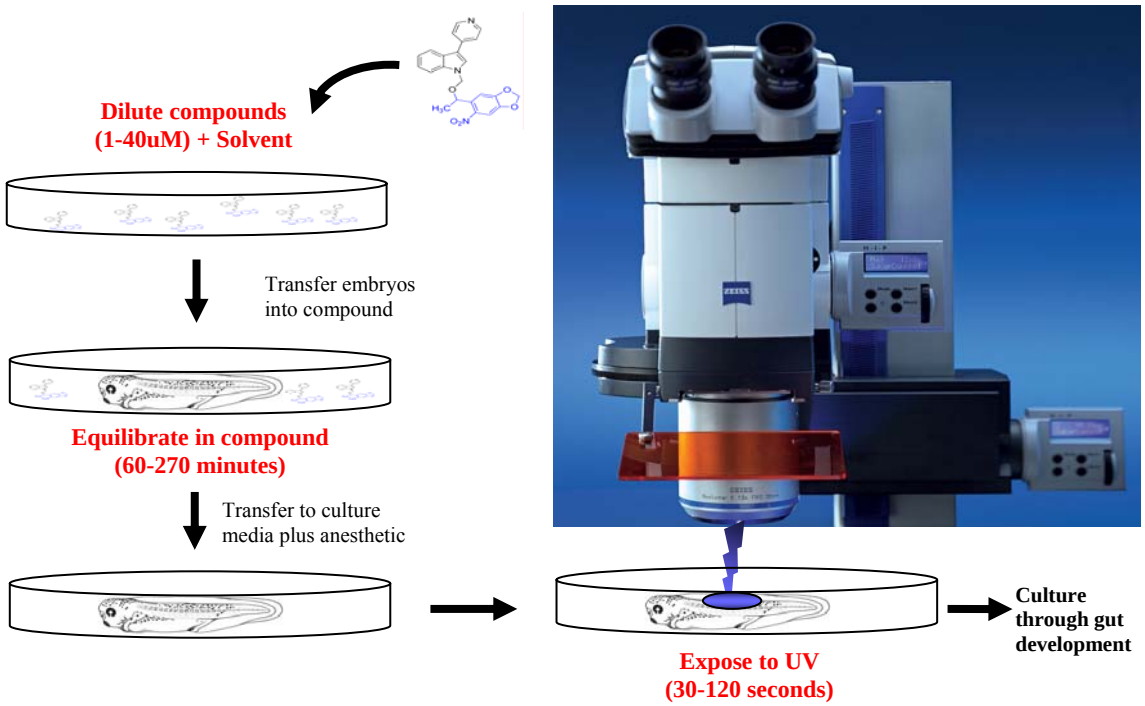

Figure 7: <u>Photoactivation of a caged ROCK inhibitor (cMRO) in *Xenopus* embryos.</u> For photoactivation, embryos were placed in dishes with pre-dispensed **MRO** or **cMRO** (or solvent) and allowed to equilibrate for short periods of time (or exposed long-term; ~3days). After equilibration, the embryos were transferred to culture media, immobilized in anesthetic and irradiated with a fluorescent stereomicroscope equipped with a mercury light source and UV (DAPI) filter to limit wavelengths to the range of 359-371nm. Embryos were then cultured for analysis of gut development. Parameters in red were optimized for *Xenopus.*

It is known that endogenous ROCK activity is required for the undeveloped *Xenopus* gut tube to elongate and rotate into a coiled intestine. Long term (~72 hours) treatment of the entire embryo with **RO** beginning at stages just prior to gut morphogenesis elicits various concentration-dependent defects in gut tube elongation and intestinal rotation (Reed et al.,

2009), with the most severe defect being a straightened, non-elongated gut tube (Figure 8A). These phenotypes can be easily visualized through the transparent abdomen of the *Xenopus* tadpole (see Figure 8). The degree of localized gut elongation defects was therefore assessed as a phenotypic readout of the efficacy of **MRO** and **cMRO** *in vivo*.

The highest solubility of **cMRO** in embryo media (0.1X MMR) was empirically determined to be 40 μM (data not shown). This concentration was used to assay the efficacy of the caged compound in living *Xenopus laevis* embryos. Long term exposure (~72 hours) to 40 μM **MRO** (Figure 8 B) resulted in embryos with non-elongated gut tubes (100%, n= 5) confirming that the hydroxymethyl derivative RO that is released upon UV exposure of **cMRO** is absorbed by *Xenopus* tissues with a similar cell permeability and elicits the same phenotype as **RO** *in vivo*.

As expected, exposure of embryos to **cMRO** in the absence of UV irradiation did not result in a gut phenotype (Figure 8E, 0%, n=5); however, exposure to **cMRO** with 1 minute UV exposure resulted in 100% of embryos exhibiting a gut elongation phenotype on the side of irradiation (Figure 8F). This phenotype was not caused by the UV exposure itself since no embryos exposed to solvent or **MRO** alone exhibited a phenotype upon exposure to the same dose/duration of UV (Figure 8D; see also Appendix, Figure A1). Importantly, LC-MS analyses indicate that, although only **cMRO** can be detected in embryo extracts kept in the dark, approximately equal intraembryonal concentrations of caged (**cMRO**) to decaged (**MRO**) compound exist in the extracts of embryos exposed to UV, confirming that UV exposure releases **MRO** *in vivo*.

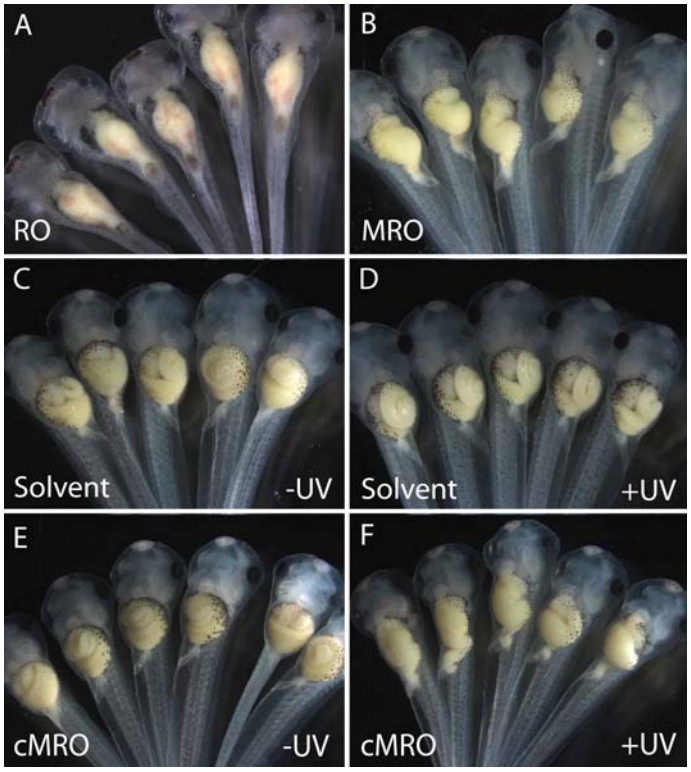

Figure 8. ***In vivo*** **efficacy of photoactivatable ROCK inhibitor is UV dependent.** The phenotype elicited upon global ROCK Inhibition is a straightened tube as seen with 40uM **RO** (A). Long-term treatment in 40µM **MRO** elicits a similar yet less severe straightened gut (B). Control treatments with solvent –UV (C) and +UV (D), and short-term treatment with **cMRO** –UV (E) elicited normal phenotypes. Upon UV irradiation, short-term treatment in **cMRO** (F) induces 100% non-elongated, straightened gut tubes. Long-term treatment was approximately 72 hours and short-term treatment was 2 hours. (n=5 for each condition)

To confirm that the gut elongation phenotype elicited from **cMRO** decaging was not due to toxicity of the released caging group, embryos were exposed to both the "pre-UV irradiation" **NPOMalc** (alcohol) form of the caging group and the "post-UV irradiation" **NPOMace** (nitroso-acetophenone) form of the caging group (see Figure 9 below; also see Figure 3). Neither exposing embryos to caging groups in the medium, nor microinjecting the caging groups directly into the embryo, caused abnormalities in the presence or absence of UV

(data not shown). Overall, these experiments illustrate that the NPOM-caged ROCK inhibitor, **cMRO,** inhibits ROCK activity in a light-controlled manner both *in vitro* and *in vivo*.

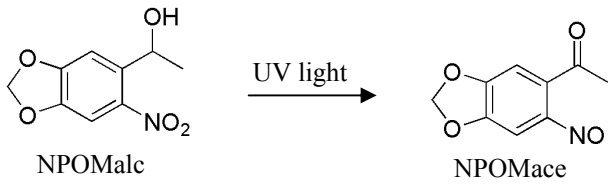

Figure 9. NPOM Scheme. Prior to irradiation the NPOM caging group is in its alcohol form NPOMalc (alcohol). Upon 365 nm UV light irradiation the caging group is transformed into its NPOMace (nitroso-acetophenone) form of the caging group

Activity of Caged-ROCK Inhibitor is UV- and Concentration Dependent

To determine the minimum/optimal concentration of **cMRO** necessary to elicit a UV-dependent ROCK-deficient gut phenotype *in vivo*, the reagent was tested for short periods of time at different concentrations, including 1, 10, 15, and 20 μM. The frequency of gut elongation phenotypes increases as the concentration of **cMRO** increases, reaching 100% at 15μM (Figure 10), while the solvent and **MRO** controls had no detectable effect on gut morphogenesis at any concentration (data not shown). These results suggest that 15 μM **cMRO** is the optimal concentration necessary to elicit a high frequency of phenotypes upon UV irradiation. A concentration of 15μM **cMRO** was used in all subsequent experiments.

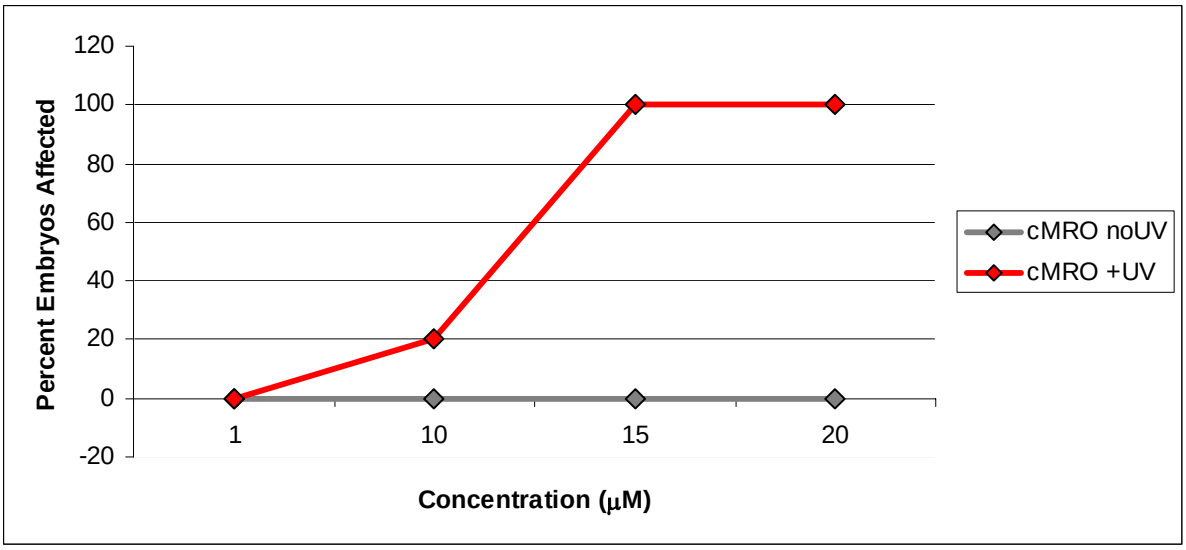

Figure 10. ***In vivo*** **efficacy of photoactivated cMRO is concentration dependent.** To determine the optimal concentration of **cMRO** to induce UV-dependent gut elongation phenotypes, embryos were exposed to solvent or 1, 10, 15, or 20 μM **MRO** or **cMRO** and either UV irradiated (+UV, 60sec) or mock irradiated (noUV). Phenotypes from short term (120min) exposure begin to be observed at 10μM while a high (100%) frequency of phenotypes occurs at both 15 and 20μM. (n=5 for each condition)

Activity of Caged-ROCK Inhibitor is Dependent on Equilibration Time

In order to determine the optimal equilibration time to elicit localized gut defects from localized ROCK inhibition, embryos were equilibrated in 15μM compound for different lengths of time before UV irradiation, from 60-270 minutes (Figure 11). A minimum equilibration time of 120 minutes was required to elicit an observable gut phenotype. At 60 and 90 minutes of equilibration there are no abnormalities (0%, n=5). At 120 minutes of equilibration, 40% "mild" (some gut straightening, none to mild edema; see Figure 11B) and 40% "severe" (extreme gut straightening, edema; see Figure 11D) gut elongation phenotypes

are elicited. At 150, 180, and 210 minutes of equilibration 80% of embryos exhibited severe phenotypes with only 10% mild phenotypes (n=5). A peak with 100% severe phenotypes was elicited upon 240 and 270 min. of equilibration. These results suggest that 120-150 minutes of equilibration yields a high frequency of ROCK inhibition with a minimal amount of severe or secondary defects. An equilibration time of 120 minutes was used in all subsequent experiments.

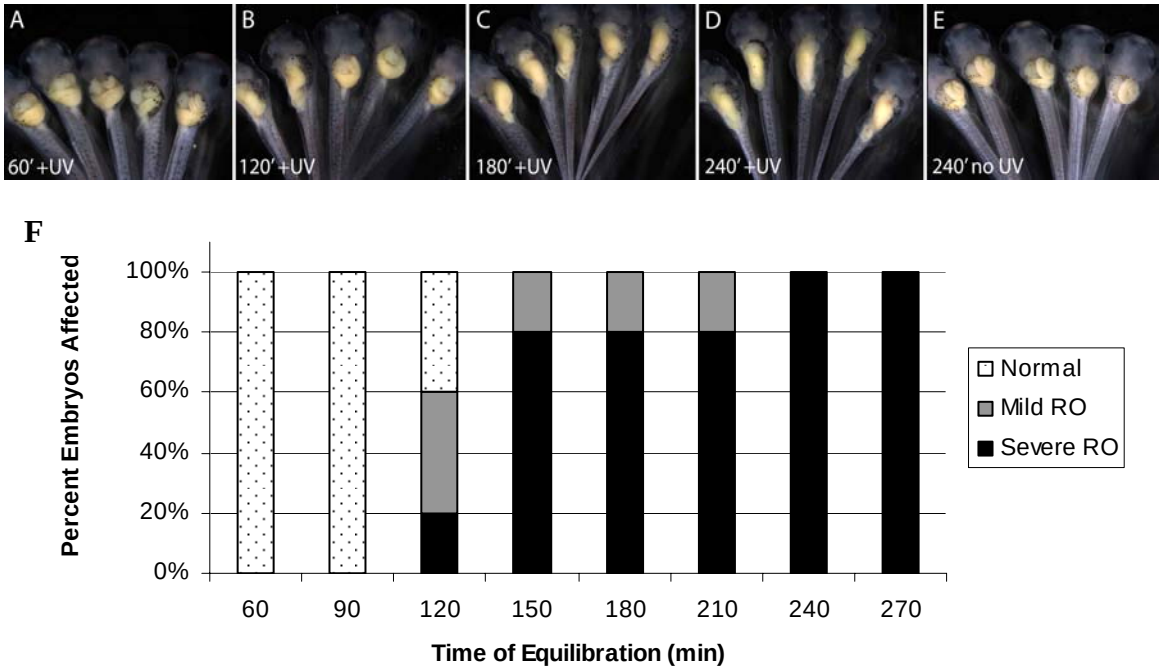

Figure 11. ***In vivo*** **efficacy of photoactivated cMRO is dependent on equilibration time.** Embryos were equilibrated in 15μM **cMRO** for 60 (A), 90, 120 (B), 150, 180 (C), 210, 240 (D, E), and 270 minutes, and then photoactivated (right side of gastrointestinal tract, A-D) or mock-irradiated (E). (F) The frequency and severity of gut elongation phenotypes increases with increasing equilibration time, peaking above 210' (n=5 for each condition). UV irradiation was 60 seconds for all equilibrations.

Activity of Caged-ROCK Inhibitor is Dependent on Length of UV Exposure

To determine the minimal UV exposure required to elicit the ROCK inhibitory activity of **cMRO**, exposure times of 30, 60, 90, and 120 seconds were tested (Figure 12). Mild gut elongation phenotypes were elicited, a frequency of 20%, when irradiated 30 seconds (Figure 12A). At 60 seconds of UV irradiation (Figure 12B), mild phenotypes increased to 40%, with 20% severe phenotypes. At 90 seconds (Figure 12C), 40% were mild phenotypes, and 40% were severe phenotypes. Then at 120 seconds of UV irradiation (Figure 12D), 100% of embryos exhibited severe abnormalities. These results suggest that at least 60 seconds of UV irradiation elicited an increased frequency of mild phenotypes with a minimal frequency of severe phenotypes, suggesting 60 seconds is the optimal time for UV irradiation. A UV exposure time of at least 60 seconds was used in all subsequent experiments.

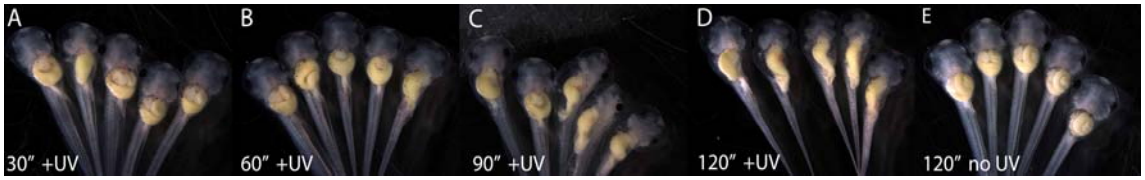

F

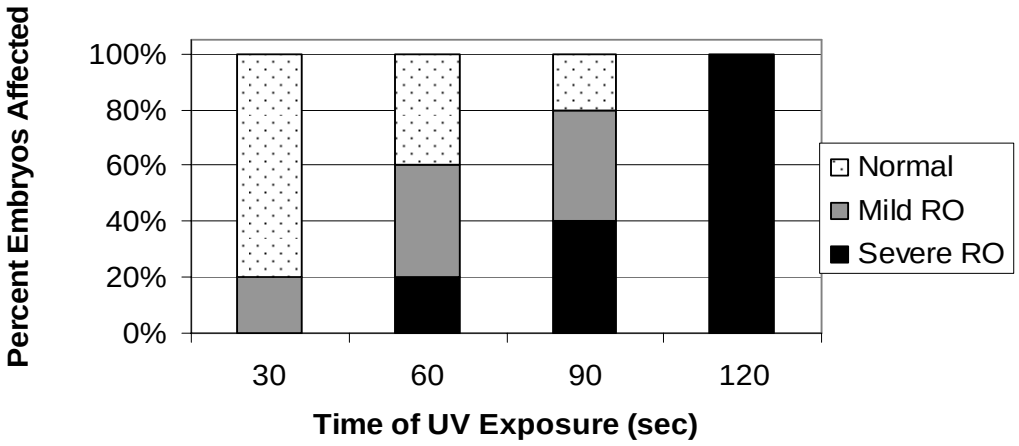

Figure 12. *In vivo* efficacy of cMRO is dependent on length of UV exposure. Embryos were equilibrated in 15μM **cMRO** (A-E), and exposed to UV (+UV) for 30 sec (A), 60 sec (B), 90 sec (C), 120 sec (D), or were mock-irradiated (no UV; E). Between the range of 60-90 seconds UV exposure, a mixture of mild and severe phenotypes are elicited, whereas 120 seconds UV exposure elicits 100% severe phenotypes. The frequency (F) and severity of abnormal gut elongation phenotypes increases with increasing UV exposure time (n=5 for each condition).

Localization of ROCK Inhibition

To confirm that the gut defects induced by photoactivation of **cMRO** correspond to the regions of the gut where **MRO** was released by UV irradiation, embryos were injected with a green-to-red photoconvertible fluorescent protein, EosFP, at the 2-4 cell stage (Wacker et al., 2007). Prior to UV exposure, this protein labels cells with green fluorescence,

which is photoconverted to red fluorescence only in the region exposed to UV irradiation. Embryos with green fluorescent cells in the gut tissue (stage 37-39) were exposed to either solvent or 15μM **cMRO** and photoactivated as above (see Methods). In embryos treated with solvent alone, the red-orange fluorescence highlights the cells that have rearranged along the length of the elongating gut tube by stage 44 (Figure 13A-A''). In contrast, the highest red-orange fluorescence in embryos exposed to **cMRO** corresponds to the areas with the disrupted cell distribution and impaired gut elongation (Figure 13B-B''and 13C- 13C''), confirming that the regions in which ROCK was inhibited upon photoactivation of **cMRO** are the regions that show the phenotype. Thus, ROCK inhibition can be successfully localized *in vivo* by photoactivation of **cMRO**, to induce localized phenotypic defects.

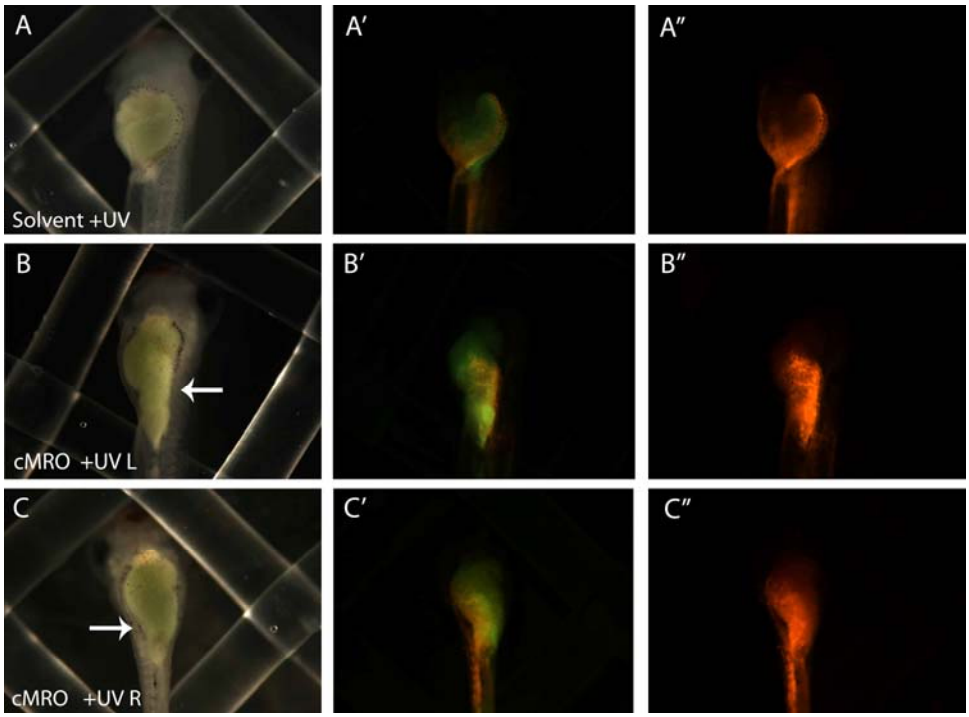

Figure 13. Irradiated site co-localizes with abnormal cell rearrangements. Embryos were injected at the 2-4 cell stage with EosFP mRNA, encoding a green fluorescent protein that converts to red fluorescence upon UV irradiation (~350nm). Injected embryos at stage 37-39 were equilibrated for 120-180 minutes in solvent(A) or 15μM **cMRO** (B,C) and UV irradiated for 60 seconds on either the left (B) or right (A,C) side. Brightfield (A, B, C), green/red fluorescent overlay images (A', B', C') and red fluorescence alone (A'', B'', C'') are shown for each embryo. Red fluorescence indicates the region of UV exposure and therefore, the tissue with ROCK inhibited; note the decreased gut elongation and disrupted cell rearrangements. Arrows indicate the side of UV irradiation.

Localized ROCK Inhibition Affects Gut Epithelial Architecture

Previous reports showed that ROCK inhibition by **RO** causes changes in gut cell shape and epithelial architecture (Reed et al., 2009). To confirm that the localized phenotypic effect of **cMRO** is caused by the expected alteration of cellular properties by ROCK inhibition, immunohistochemistry was performed on sections of **cMRO** treated embryos with and without UV photoactivation (Figure 14A). In embryos kept in the dark,

and thus not subject to ROCK inhibition, the cellular architecture reflects the normal polarized columnar epithelium that lines the intestine. In contrast, in photoactivated embryos (Figure 8B-C), the side that was UV irradiated corresponds to the side in which cells are abnormally rounded, and the cellular architecture is non-polarized and disorganized. Importantly, the non-irradiated side maintains the normal polarized columnar epithelium. These results confirm that the expected cellular changes caused by ROCK inhibition are achieved in a localized manner in response to localized photoactivation of **cMRO** *in vivo*.

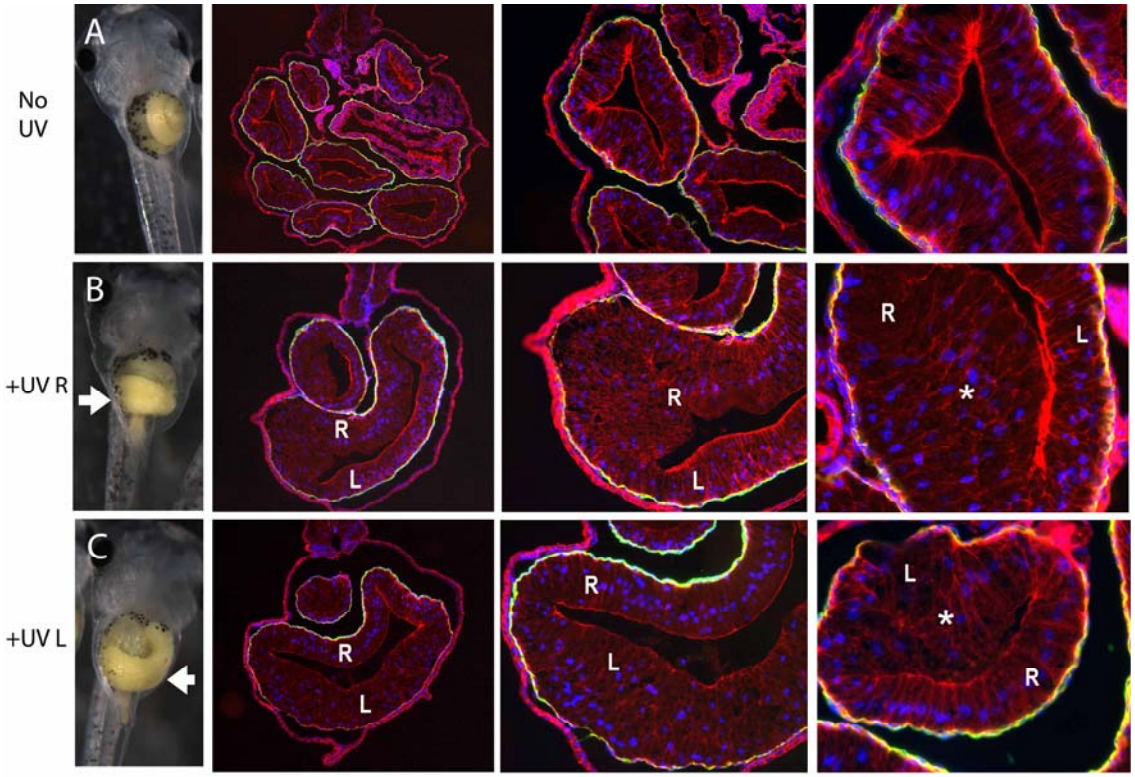

Figure 14. Cellular architecture is locally disrupted by photoactivation of cMRO. Embryos were equilibrated for 120-180 min. in 15μM **cMRO** and mock irradiated (A) or UV irradiated for 60 seconds on either the right (B) or left side (C), cultured through gut morphogenesis, fixed, and cryosectioned. Sections were immunohistochemically stained to visualize smooth muscle actin (red), βeta-catenin (green), and nuclei (DAPI, blue). Arrows indicate the side that was UV irradiated. Epithelial architecture was locally perturbed, indicated by *, by photoactivation of **cMRO**. Images increase in magnification from left to right; 10X, 20X, 40X.

DISCUSSION

Only a limited number of genetic and chemical tools are available to investigate complex late stage morphogenetic processes like gut organogenesis. In order to fully investigate such processes in living embryos, spatially and temporally controlled loss of function strategies are required. While perturbation of signaling components with small molecule inhibitors can bypass earlier developmental processes in which the targeted signaling pathway is also required, the entire embryo is exposed to the compound increasing the risk for pleiotropic deformities or off-target effects. In this thesis, a photoactivatable small molecule inhibitor of ROCK activity was developed, and optimal parameters for its use in living *Xenopus laevis* embryos were determined.

Upon UV irradiation of a NPOM-caged ROCK inhibitor (**cMRO**), a hydroxymethyl derivative (**MRO**) was released. Like **RO**, this novel compound was found to be an effective inhibitor of ROCK both *in vitro* and *in vivo*. Although optimal photoactivation parameters for interrogating gut morphogenesis with **cMRO** were identified herein, each parameter (equilibration time, UV exposure, concentration of caged compound) can be adjusted independently, if necessary, for studying alternate organs or tissues at different stages of development. It should be noted that, although only a brief (2 hr) equilibration is required to elicit desired UV-dependent phenotypic effects in the developing gut tube, **cMRO** appears to be slightly unstable in the absence of irradiation, causing mild gut defects in embryos exposed to the caged compound at high concentrations (40μM) over long periods of time

(~3 days; data not shown). Photoactivation of embryos exposed to high concentrations of **cMRO** can also cause additional developmental defects, such as edema. These effects may result from other processes such as angiogenesis being specifically disrupted by ROCK inhibition (Fischer et al., 2009), or may be the result of off-target activity. For these reasons, the caged compound should only be used at minimal concentrations and equilibration times to achieve light-dependent phenotypic outcomes.

Although exposure to **cMRO** for as little as two hours is sufficient to elicit an obvious phenotype upon UV exposure, similar exposure to the active uncaged compound (**MRO)** itself for the same equilibration time does not induce any abnormalities (see Appendix, Figure A2). This seemingly paradoxical result suggests that the hydroxymethyl group on **MRO** may result in decreased cell permeability compared to **RO**, while the NPOM-caging group may actually allow the **MRO** to diffuse into the embryonic cells more easily. Upon irradiation, the now decaged **MRO** compound is released *in vivo*, and thus returned to its less permeable form, effectively trapping **MRO**-mediated ROCK inhibitory activity inside the irradiated cells, where it elicits severe effects. Indeed, this hypothesis is supported by LC-MS data which indicates that under the same conditions almost three-fold more **cMRO** diffuses into the embryo than **MRO** (~45μM cMRO vs. ~14μM MRO).

This study shows that the use of light-responsive molecules such as **cMRO** can be a powerful method of modulating and analyzing developmental processes in *Xenopus* embryos. In addition to confirming the applicability of caged compounds in living embryos, this study illustrates how the UV light source from a standard fluorescent stereomicroscope can be used

as a decaging system to make photoregulation less expensive and more widely accessible to the average developmental biology lab. In the future, **cMRO** can be used to achieve more precise ROCK perturbation along the length of the gut tube, in specific populations of gastrulating cells, or in other Rho-dependent developmental processes in *Xenopus* embryos. Of course, the use of **cMRO** or other photocaged inhibitors is not restricted to use in *Xenopus* species; this technique is generally applicable to other embryos and tissues, as well as in defined populations of cultured cells.

REFERENCES

1. 1994. Normal table of Xenopus Laevis (Daudin): a systematical and chronological survey of the development from fertilized egg till the end of metamorphosis. Garland Publishing, INC. Editors **Nieuwkoop and Faber**.

2. **Adams S. R., and R. Y. Tsien**. 1993. Controlling Cell Chemistry with Caged Compounds. Annu. Rev. Physiol. **55**:755-784.

3. **Amano M.** 2000. Regulation and Functions of Rho-Associated Kinase. Experimental Cell Research **261**:44-51.

4. **Asanuma, Liang, Yoshida, Yamazawa, and Komiyama**. 2000. Photocontrol of Triple-Helix Formation by Using Azobenzene-Bearing Oligo(thymidine) This work was partially supported by a Grant-in-Aid for Scientific Research from the Ministry of Education, Science, and Culture, Japan (Molecular Synchronization for the Design of New Material Systems). The grant from the "Research for the Future" program of the Japanese Society for the Promotion of Science (JSPS-RFTF97I00301) is also acknowledged. Angew. Chem. Int. Ed. Engl **39**:1316-1318.

5. **Callaway E. M., and R. Yuste**. 2002. Stimulating neurons with light. Curr. Opin. Neurobiol **12**:587-592.

6. **Chalmers A. D., and J. M. Slack**. 2000. The Xenopus tadpole gut: fate maps and morphogenetic movements. Development **127**:381-392.

7. **Cook B. N., and C. R. Bertozzi**. 2002. Chemical approaches to the investigation of cellular systems. Bioorg. Med. Chem **10**:829-840.

8. **Corrie J. E. T., A. Barth, V. R. N. Munasinghe, D. R. Trentham, and M. C. Hutter**. 2003. Photolytic cleavage of 1-(2-nitrophenyl)ethyl ethers involves two parallel pathways and product release is rate-limited by decomposition of a common hemiacetal intermediate. J. Am. Chem. Soc **125**:8546-8554.

9. **Cruz F. G., J. T. Koh, and K. H. Link**. 2000. Light-Activated Gene Expression. J. Am. Chem. Soc. **122**:8777-8778.

10. **Deiters A., R. A. Garner, H. Lusic, J. M. Govan, M. Dush, N. M. Nascone-Yoder, and J. A. Yoder**. 2010. Photocaged Morpholino Oligomers for the Light-Regulation of Gene Function in Zebrafish and Xenopus Embryos. Journal of the American Chemical Society **132**:15644-15650.

11. **Dong Q., K. Svoboda, T. Tiersch, and W. Toddmonroe**. 2007. Photobiological effects of UVA and UVB light in zebrafish embryos: Evidence for a competent photorepair system. Journal of Photochemistry and Photobiology B: Biology **88**:137-146.

12. **Dormán G., and G. D. Prestwich**. 2000. Using photolabile ligands in drug discovery and development. Trends Biotechnol **18**:64-77.

13. **Etienne-Manneville S., and A. Hall**. 2002. Rho GTPases in cell biology. Nature **420**:629-635.

14. **Furuta T., and M. Iwamura**. 1998. New caged groups: 7-substituted coumarinylmethyl phosphate esters. Meth. Enzymol **291**:50-63.

15. **Furuta T., S. S. Wang, J. L. Dantzker, T. M. Dore, W. J. Bybee, E. M. Callaway, W. Denk, and R. Y. Tsien**. 1999. Brominated 7-hydroxycoumarin-4-ylmethyls: photolabile protecting groups with biologically useful cross-sections for two photon photolysis. Proc. Natl. Acad. Sci. U.S.A **96**:1193-1200.

16. **Givens R. S., J. F. Weber, A. H. Jung, and C. H. Park**. 1998. New photoprotecting groups: desyl and p-hydroxyphenacyl phosphate and carboxylate esters. Meth. Enzymol **291**:1-29.

17. **Goard M., G. Aakalu, O. D. Fedoryak, C. Quinonez, J. St. Julien, S. J. Poteet, E. M. Schuman, and T. M. Dore**. 2005. Light-Mediated Inhibition of Protein Synthesis. Chemistry & Biology **12**:685-693.

18. **Goeldner M., and R. Givens**. 2005. Dynamic studies in biology: phototriggers, photoswitches and caged biomolecules. Wiley-VCH.

19. **Hagen V., S. Frings, B. Wiesner, S. Helm, U. B. Kaupp, and J. Bendig**. 2003. [7-(Dialkylamino)coumarin-4-yl]methyl-Caged Compounds as Ultrafast and Effective Long-Wavelength Phototriggers of 8-Bromo-Substituted Cyclic Nucleotides. Chembiochem **4**:434-442.

20. **Kaplan J. H., B. Forbush, and J. F. Hoffman**. 1978. Rapid photolytic release of adenosine 5'-triphosphate from a protected analog: utilization by the sodium:potassium pump of human red blood cell ghosts. Biochemistry **17**:1929-1935.

21. **Kawasumi M., and P. Nghiem**. 2007. Chemical Genetics: Elucidating Biological Systems with Small-Molecule Compounds. J Investig Dermatol **127**:1577-1584.

22. **Lee T. H., K. R. Gee, C. Davidson, and E. H. Ellinwood**. 2002. Direct, real-time assessment of dopamine release autoinhibition in the rat caudate-putamen. Neuroscience **112**:647-654.

23. **Li H., J. Hah, and D. S. Lawrence**. 2008. Light-mediated liberation of enzymatic activity: "small molecule" caged protein equivalents. J. Am. Chem. Soc **130**:10474-10475.

24. **Liang X., T. Yoshida, H. Asanuma, and M. Komiyama**. 2000. Photo-regulation of DNA/RNA duplex formation by azobenzene-tethered DNA towards antisense strategy. Nucleic Acids Symp. Ser 277-278.

25. **Lin W., C. Albanese, R. G. Pestell, and D. S. Lawrence**. 2002. Spatially discrete, light-driven protein expression. Chem. Biol **9**:1347-1353.

26. **Link K. H., Y. Shi, and J. T. Koh**. 2005. Light Activated Recombination. J. Am. Chem. Soc. **127**:13088-13089.

27. **Lipscomb K., C. Schmitt, A. Sablyak, J. A. Yoder, and N. Nascone-Yoder**. 2006. Role for retinoid signaling in left-right asymmetric digestive organ morphogenesis. Dev. Dyn **235**:2266-2275.

28. **Lusic H., and A. Deiters**. 2006. A New Photocaging Group for Aromatic N - Heterocycles. Synthesis **2006**:2147-2150.

29. **Lusic H., D. D. Young, M. O. Lively, and A. Deiters**. 2007. Photochemical DNA activation. Org. Lett **9**:1903-1906.

30. **Maier W., J. E. T. Corrie, G. Papageorgiou, B. Laube, and C. Grewer**. 2005. Comparative analysis of inhibitory effects of caged ligands for the NMDA receptor. J. Neurosci. Methods **142**:1-9.

31. **Marriott G., and J. Ottl**. 1998. Synthesis and applications of heterobifunctional photocleavable cross-linking reagents. Meth. Enzymol **291**:155-175.

32. **Mayer G., and A. Heckel**. 2006. Biologically Active Molecules with a “Light Switch”. Angew. Chem. Int. Ed. **45**:4900-4921.

33. **McCray J. A., and D. R. Trentham**. 1989. Properties and uses of photoreactive caged compounds. Annu Rev Biophys Biophys Chem **18**:239-270.

34. **Muller J. K., D. R. Prather, and N. M. Nascone-Yoder**. 2003. Left-right asymmetric morphogenesis in the Xenopus digestive system. Dev. Dyn **228**:672-682.

35. **Neveu P., I. Aujard, C. Benbrahim, T. Le Saux, J. Allemand, S. Vriz, D. Bensimon, and L. Jullien**. 2008. A Caged Retinoic Acid for One- and Two-Photon Excitation in Zebrafish Embryos. Angew. Chem. Int. Ed. **47**:3744-3746.

36. **Ouyang X., and J. K. Chen**. 2010. Synthetic Strategies for Studying Embryonic Development. Chemistry & Biology **17**:590-606.

37. **Pelliccioli A. P., and J. Wirz**. 2002. Photoremovable protecting groups: reaction mechanisms and applications. Photochem. Photobiol. Sci **1**:441-458.

38. **Pillai R. P., F. M. Raushel, and J. J. Villafranca**. 1980. Stereochemistry of binding of thiophosphate analogs of ATP and ADP to carbamate kinase, glutamine synthetase, and carbamoyl-phosphate synthetase. Arch. Biochem. Biophys **199**:7-15.

39. **Pillai S., and B. K. Bachhawat**. 1979. Affinity immobilisation and "negative" crosslinking: a probe for tertiary and quaternary protein structure. J. Mol. Biol **131**:877-881.

40. **Raftopoulou M., and A. Hall**. 2004. Cell migration: Rho GTPases lead the way. Dev. Biol **265**:23-32.

41. **Redowicz M. J.** 1999. Rho-associated kinase: involvement in the cytoskeleton regulation. Arch. Biochem. Biophys **364**:122-124.

42. **Reed R. A., M. A. Womble, M. K. Dush, R. R. Tull, S. K. Bloom, A. R. Morckel, E. W. Devlin, and N. M. Nascone-Yoder**. 2009. Morphogenesis of the primitive gut tube is generated by Rho/ROCK/myosin IIâ “mediated endoderm rearrangements. Dev. Dyn. **238**:3111-3125.

43. **Riento K., and A. J. Ridley**. 2003. Rocks: multifunctional kinases in cell behaviour. Nat. Rev. Mol. Cell Biol **4**:446-456.

44. **Settleman J.** 2001. Rac 'n Rho: the music that shapes a developing embryo. Dev. Cell **1**:321-331.

45. **Shestopalov I. A., S. Sinha, and J. K. Chen**. 2007. Light-controlled gene silencing in zebrafish embryos. Nat Chem Biol **3**:650-651.

46. **Sive H., R. Grainger, and R. Harland**. 1998. Early development of Xenopus laevis: A laboratory manual. Cold Spring Harbor Laboratory Press.

47. **Soderholm J., and R. Heald**. 2005. Scratch n' Screen for Inhibitors of Cell Migration. Chemistry & Biology **12**:263-265.

48. **Stockwell B. R.** 2000. Chemical genetics: ligand-based discovery of gene function. Nat. Rev. Genet **1**:116-125.

49. **Suzuki A. Z., T. Watanabe, M. Kawamoto, K. Nishiyama, H. Yamashita, M. Ishii, M. Iwamura, and T. Furuta**. 2003. Coumarin-4-ylmethoxycarbonyls as phototriggers for alcohols and phenols. Org. Lett **5**:4867-4870.

50. **Symons M., and J. Settleman**. 2000. Rho family GTPases: more than simple switches. Trends Cell Biol **10**:415-419.

51. **Takaoka K., Y. Tatsu, N. Yumoto, T. Nakajima, and K. Shimamoto**. 2003. Synthesis and photoreactivity of caged blockers for glutamate transporters. Bioorg. Med. Chem. Lett **13**:965-970.

52. **Takaoka K., Y. Tatsu, N. Yumoto, T. Nakajima, and K. Shimamoto**. 2004. Synthesis of carbamate-type caged derivatives of a novel glutamate transporter blocker. Bioorg. Med. Chem **12**:3687-3694.

53. **Wacker S. A., F. Oswald, J. Wiedenmann, and W. Knöchel**. 2007. A green to red photoconvertible protein as an analyzing tool for early vertebrate development. Dev. Dyn. **236**:473-480.

54. **Yarrow J. C., G. Totsukawa, G. T. Charras, and T. J. Mitchison**. 2005. Screening for Cell Migration Inhibitors via Automated Microscopy Reveals a Rho-Kinase Inhibitor. Chemistry & Biology **12**:385-395.

55. **Yeh J. J., and C. M. Crews**. 2003. Chemical genetics: adding to the developmental biology toolbox. Dev. Cell **5**:11-19.

56. **Young D. D., and A. Deiters**. 2007. Photochemical control of biological processes. Org. Biomol. Chem. **5**:999.

APPENDICES

Appendix 1.

Short-term treatment with MRO

Objective

The objective of this experimental group was to control for effects from UV exposure and compound interactions.

Methods

Embryos were cultured to st.37-39 then treated in 40µM **MRO** short-term (2 hours) before being UV irradiated (+UV) for 60 seconds or mock irradiated (no UV). Then embryos were incubated in fresh 0.1X MMR at 18.5-23ºC in the dark until scoring stage (st.43-45).

Results and Discussion

Although exposure to **cMRO** for 2 hrs is sufficient to elicit an obvious phenotype upon UV exposure, similar exposure to the active uncaged compound (**MRO)** itself for 2 hrs does not induce any abnormalities with or without exposure to UV irradiation. This is comparable to what is seen with short-term treatment in **RO**.

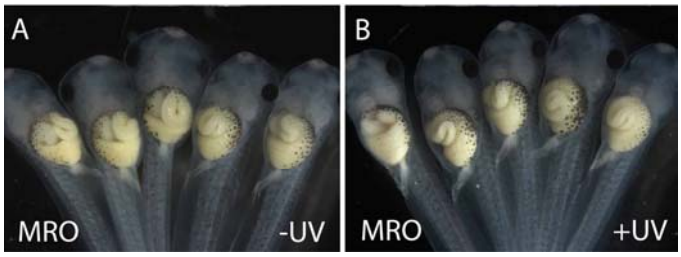

Figure A1. Short-term equilibration with MRO does not perturb gut development in *Xenopus* embryos. As additional negative controls, embryos were also treated short-term (2 hours) with 40µM **MRO** and either mock irradiated (–UV; **A**) or UV irradiated (+UV; **B**). Both groups elicited all normal phenotypes (100%). (n=5 for both UV conditions)

Appendix 2.

Long-term treatment with cMRO

Objective

The objective of this experiment was to determine the long-term effect of **cMRO** treatment on *Xenopus* embryos.

Methods

Embryos were treated long-term (~3days) with **cMRO** at 1, 10, 15, 20 µM starting at a stage prior to gut development (st.37/38). The compound was dispensed into 0.1X MMR prior to adding embryos and then incubated at 18.5-23ºC in the dark until scoring stage (st.43-45).

Results and Discussion

With long-term exposure to **cMRO**, 20µM elicited 100% elongation defects as was seen with 40µM treatment. Long-term exposure at lower concentrations, however, did not elicit any gut defects (Figure A2), nor did long-term exposure to solvent or **MRO**. These results indicate long-term instability of **cMRO** at concentrations of 20µM or higher.

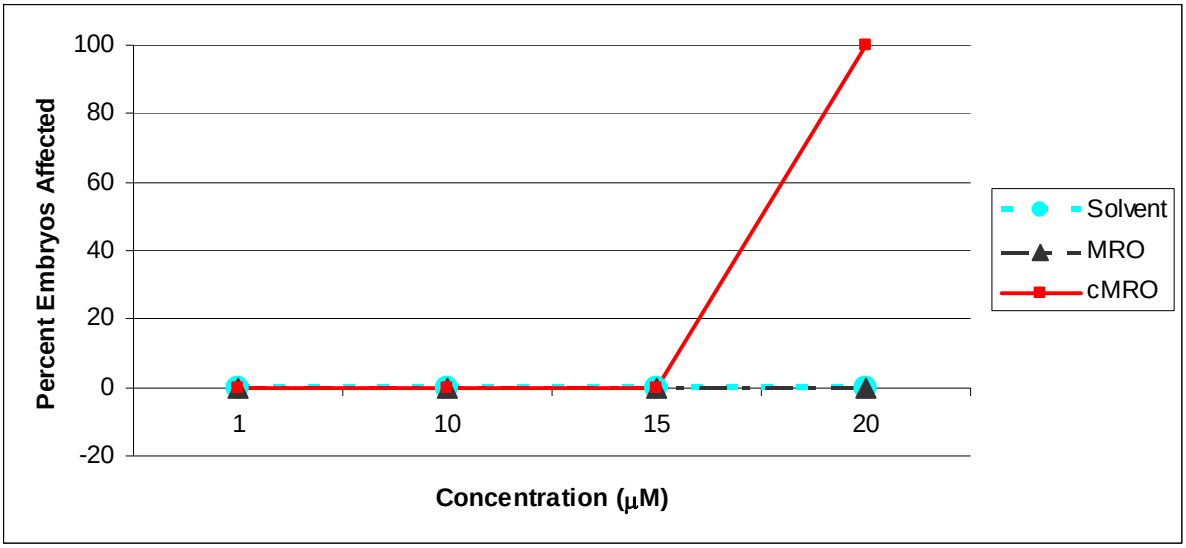

Figure A2. cMRO is unstable over long periods of time. To determine the optimal concentration of **cMRO** to induce UV-dependent gut phenotypes, embryos were exposed long-term (~72 hours) to solvent or 1, 10, 15, or 20μM **MRO** or **cMRO** and were kept in the dark. Phenotypes from long-term exposure are minimal at 15μM but increase to 100% abnormal gut elongation phenotypes with an increase in concentration to 20μM. This suggests instability of **cMRO** at high concentrations (>15μM) and long-term exposure. (n=5 for each condition)